Entanglement of electron spins and geometric phases in the diamond color center coupled to the P1 center

M. Hebbache

Université Denis Diderot, Sorbonne Paris Cité, MPQ, UMR 7162 CNRS, F-75205 Paris, France

Impurity spins in semiconductors are potential quantum bits. Entanglement and topological phases are key resources in quantum computation. We prove that the coupled electron spins carried by a diamond nitrogen-vacancy color center (NV$^-$) and a single substitutional nitrogen impurity (P1 center) are entangled in the immediate vicinity of the level anticrossing that appears in the Zeeman energy diagram at about 500 G. We also determine the Aharonov-Anandan, Berry, and marginal geometric phases that can be accumulated by the state vectors of this spin system when it is magnetically transported around a closed path. At the resonance where the gap between two energy levels is minimum, the geometric phases undergo discontinuities, and the entanglement of the two electron spins is maximal.

I. INTRODUCTION

Since the proposal of Kane,[1] impurity spins in solids have received great attention as quantum bits (qubits) for the realization of a solid-state quantum computer. The electron spin 1 carried by the negatively charged nitrogen-vacancy (NV$^-$) color center of diamond is probably the most promising candidate for a qubit.[2] The control of the interactions with its environment and, in particular, with the electron spin $\frac{1}{2}$ carried by the P1 center, a nitrogen atom in a substitutional position, is progressing.[3,4] Modeling these interactions is a major challenge.

In a previous work,[5] an effective spin Hamiltonian was built for investigating the energy spectrum of the NV$^-$-P1 coupled defect pair subjected to an external magnetic field. The occurrence of several level anticrossings (LAC) in the Zeeman energy diagram has been reported. The LAC that appear at about 500 and 1000 G had already been detected experimentally.[4,6] A LAC is a coupled two-level system that can be studied rigorously in the framework of the Landau-Zener theory.[5] On approaching a resonance very slowly (adiabatically), at which two energy levels are closest to one another, the coupled spins can flip individually or in concert, offering possibilities to implement quantum logic gates, which are fundamental components of a quantum computer.[4] Two-qubit quantum gates have recently been realized using the NV$^-$ electron spin coupled to the host N nuclear spin.[7] Previous achievements of quantum operations are recalled in Ref. 8.

In the present work, we prove that the electron spins carried by this coupled defect pair are actually entangled in the immediate vicinity of the resonances. This method of generation of entangled states via LAC is well known. The deep meaning of the entanglement was given by Schödinger in a three-part series.[9] Currently, this particular correlation between quantum subsystems is highly desired because it is a key resource in quantum information processing. Deutsch first showed how to exploit this phenomenon to perform quantum computation.[10]

It is well known that the state vectors of a spin system may acquire phases of geometric character if it is magnetically transported around a path in the parameter space.[11] Despite the strong anisotropy of the spin-spin interactions, a theoretical effort has been made for computing both the geometric phase accumulated by the whole spin system during a cyclic evolution[11,12] and the marginal geometric phases gained by the subsystems.[13] The motivation arose from the fact that logic phase gates can form a robust basis of a geometric quantum computer because they only depend on the areas in parameter space.[14] Any error leaves these areas invariant.

The outline of this paper is as follows. In the next section, the theoretical framework is briefly reviewed. This step mainly consists of building a Hamiltonian that includes the relevant spin-spin interactions. This model is applied in Sec. III for investigating the above-mentioned quantum phenomena, i.e., entanglement and topological phases.

II. MODEL

Diamond is a wide-band-gap material belonging to the group IV semiconductors. The face-centered-cubic unit cell contains eight carbon atoms. Each atom has four nearest neighbors in a tetrahedral arrangement. The shortest interatomic distance is 1.54 Å. During the last two decades, significant progress has been made in the investigation of its optically active structural defects (see, for example, Refs. 6 and 15). For later use, the model developed in Ref. 5 is reviewed below. The electron spin of the P1 center interacts with the nuclear spin and with the electronic spin of the NV$^-$ color.

In Refs. 4, 5, 15, and 16, these magnetic interactions have been grouped in the following Hamiltonian:

$$\mathcal{H}_1 = D\left[\left(S_z^{\mathrm{NV}}\right)^2 - \tfrac{1}{3}(S^{\mathrm{NV}})^2\right] + S^{\mathrm{NV}} \cdot J \cdot S^N + S^N \cdot A \cdot I^N, \tag{1}$$

where S^{NV}, S^N, and I^N are, respectively, the electron spin-1 operator of the color center, the electron spin-$\frac{1}{2}$ operator, and the nuclear spin-1 operator of the P1 center. $D = 2.88$ GHz is the zero-field splitting of the electronic triplet, J is the fine-structure tensor, and A is the hyperfine tensor. The independent components of J and A are given below. Due to the smallness of some parameters,[17] the corresponding parts of the spin Hamiltonian will be neglected. These are the N-related hyperfine coupling constant in the NV$^-$ defect compared with that of the isolated P1 center (less than 3 MHz instead of about

97 MHz) and the quadrupole splitting (-5 MHz). The color center lies along the threefold symmetry axis, i.e., the $\langle 111 \rangle$ crystallographic direction of the diamond structure, which is chosen as the z axis. We assume that this axial symmetry is preserved despite local strain-induced deformations of the diamond lattice.[18] The origin of the Cartesian coordinates x, y, and z is halfway between the vacancy (V) and the nitrogen impurity (N). The two defects lie within the yz plane.[16] With respect to the crystallographic axes, if the nitrogen atom is placed at the site $(0, 0, 0)$, the vacancy will be at $(\frac{1}{4}, \frac{1}{4}, \frac{1}{4})$, and the P1 center will be at $(2, 2, \overline{2})$. The Hamiltonian that describes the interaction between the spin system and an external magnetic field H applied along the direction defined by the unit vector n is of the form

$$\mathcal{H}_Z = \omega_L n \cdot (S^{\mathrm{NV}} + S^N), \qquad (2)$$

where $\omega_L = g\mu_B \|H\|$ is the Larmor frequency, g is the isotropic electronic factor, and μ_B is the Bohr magneton. The nuclear Zeeman energy is negligible (see Ref. 17).

The relative distance between the two defects varies from sample to sample but does not drastically change the Zeeman energy diagram. Nevertheless, the number, the position, and the tunnel splitting of the LAC can vary. In Ref. 5, the P1 center was placed at a distance $r = 12.12$ Å and a polar angle of $106°$. In this configuration, the symmetric tensor J has four nonzero components:[15,16]

$$J_{yy} = \xi \left(1 - \frac{3y^2}{r^2} \right), \quad J_{zz} = \xi \left(1 - \frac{3z^2}{r^2} \right), \quad J_{yz} = -\xi \frac{3yz}{r^2}, \qquad (3)$$

with $\xi = J_{xx} = g^2\mu_B^2/r^3$. Due to the axial symmetry, the tensor A has only two independent components: $A_\| = A_{zz} = 114.0$ MHz and $A_\perp = A_{xx} = A_{yy} = 81.3$ MHz.[6]

The 18-dimensional energy matrix is obtained by rewriting the total Hamiltonian $(\mathcal{H}_1 + \mathcal{H}_Z)$ in the basis $\{|m_S^{\mathrm{NV}} m_S^N m_I^N\rangle\}$. The three quantum numbers m_S^{NV}, m_S^N, and m_I^N are eigenvalues of the z component of the spin operators. The Hermitian energy matrix is almost block diagonalized in three six-dimensional blocks, which differ only by the value of m_I^N. It also contains 12 off-block elements equal to $A_\perp/2$. In the absence of an external magnetic field, the low triangle of a block is of the form

$$
\begin{pmatrix}
\Uparrow\uparrow m_I^N & \Uparrow\downarrow m_I^N & \Downarrow\uparrow m_I^N & \Downarrow\downarrow m_I^N & 0\uparrow m_I^N & 0\downarrow m_I^N \\
a+e & & & & & \\
d & b-e & & & & \\
0 & 0 & b+e & & & \\
0 & 0 & -d & a-e & & \\
d' & f & -d' & g & c+e & \\
g & -d' & f & d' & 0 & c-e
\end{pmatrix},
$$

with $a = \frac{1}{3}D - \frac{1}{2}J_{zz}$, $b = \frac{1}{3}D + \frac{1}{2}J_{zz}$, $c = -\frac{2}{3}D$, $d = \sqrt{2}d' = i\frac{1}{2}J_{yz}$, $e = \frac{1}{2}m_I^N A_\|$, $f = \frac{1}{2\sqrt{2}}J_{zz}$ and $g = \frac{1}{2\sqrt{2}}(J_{xx} - J_{yy})$. The state of a spin is represented by an arrow. A single upward (downward) arrow stands for the spin state $\frac{1}{2}$ $(-\frac{1}{2})$, and a double upward (downward) arrow stands for the state 1 (-1).

We used different methods to solve this large sparse eigenvalue problem.[19] We found that the hyperfine coupling constant $A_\perp$ changes the energy levels only slightly. The
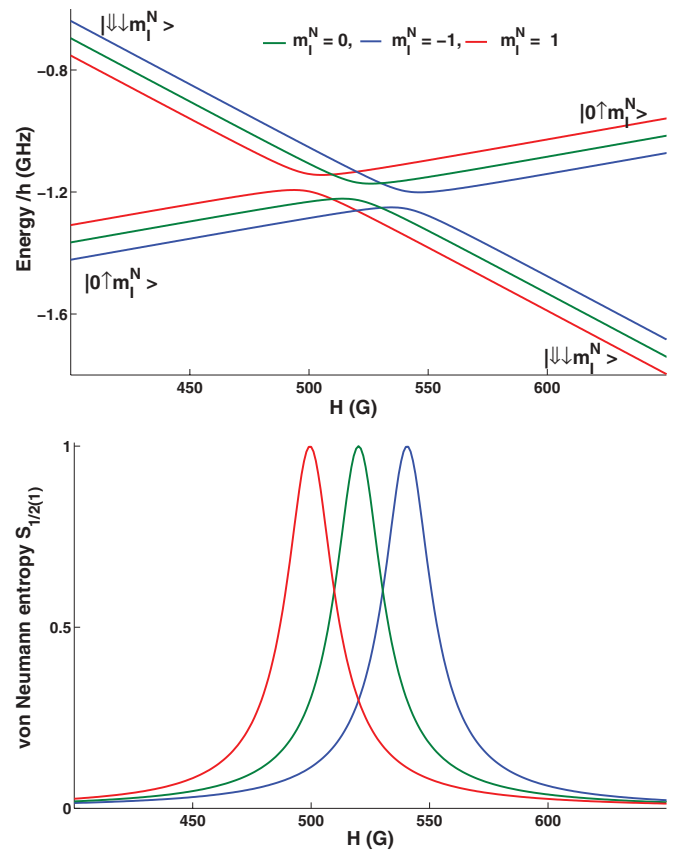

FIG. 1. (Color online) (top) Level anticrossings of the NV$^-$-P1 coupled defect pair around 500 G.[5] The spin flips are shown. A single upwards (downwards) arrow stands for the spin state $\frac{1}{2}$ $(-\frac{1}{2})$, and a double upwards (downwards) arrow stands for state 1 (-1). (bottom) The von Neumann quantum entropy $S_{\frac{1}{2}}$ $(=S_1)$ of the electron spins with respect to the strength of the magnetic field. The two electron spins are maximally entangled at the resonances.

omission of $A_\perp$ leads to the Zeeman energy diagram shown in Fig. 1 of Ref. 5. The magnetic field was applied along the direction $n = (0,0,1)$, i.e., parallel to the z axis. It lifts the twofold degeneracy of the energy levels. The energy spectrum exhibits several LAC where two energy levels approach a minimum distance. For later use, the LAC that occur around 500 G are reported in Fig. 1.

Far from the resonances, the spin system can be initially prepared in the separable state $|\psi_-\rangle = |0\uparrow m_I^N\rangle$ (see the experimental details in Refs. 3 and 4). On approaching the resonances the spin states become mixed: $|\psi_\pm\rangle = c_{1\pm} |\Downarrow\downarrow m_I^N\rangle \pm c_{2\pm} |0\uparrow m_I^N\rangle$. The $+ (-)$ sign refers to the upper (lower) energy level (Fig. 1). Above the resonances, the spin flips occur only if the quantum system is transported infinitely slowly (adiabatically). The probability transition $\|c_{J\pm}\|^2$, $J = 1$–2, can be predicted rigorously in the framework of the Landau-Zener model.[5]

Below, we show that the two electron spins are actually entangled in the immediate vicinity of the resonances. This is a theoretical demonstration of entanglement of electron spins in diamond. Of course, its practical realization is a challenge. The previous experimental demonstration of bipartite and tripartite entanglement in diamond is due to the Stuttgart group.[20] The

authors used a register of three qubits: two ^{13}C nuclear spins $\frac{1}{2}$ and the electron spin 1 of the NV$^-$ center. Nevertheless, some doubts have been raised by Lovett and Benjamin[21] (see also the response to the comment).[20]

We also investigate the geometric phases accumulated by the whole system subjected to a rotating magnetic field and extract those acquired by the subsystems. A few months ago, Maclaurin *et al.*[22] proposed two scenarios for measuring the geometric phases accumulated by the $m_S^{\mathrm{NV}} = \pm 1$ states of a single nitrogen-vacancy defect.

Entanglement and topological phases are two distinct phenomena. Indeed, a geometric phase may be generated magnetically in a single spin state while entanglement is a correlation between at least two subsystems. Nevertheless, the two phenomena can coexist in a spin system, as shown in the present work. Studies that attempt to establish a connection between them are progressing (see, for example, Ref. 23).

III. APPLICATIONS

A. Entanglement

In the literature, several methods are used to characterize the degree of entanglement between quantum subsystems: Schmidt number, tangle, concurrence, etc. An overview about the entanglement measures can be found in Ref. 24. Here, we consider the von Neumann quantum entropy, which is a generalization of the classical Shannon entropy. For a tripartite system ABC, the entropy of the subsystem A is defined as follows:

$$S_A = -\operatorname{Tr}(\rho_A \log_2 \rho_A), \tag{4}$$

where $\rho_A = \operatorname{Tr}_{BC}(|\psi_{ABC}\rangle\langle\psi_{ABC}|)$ is the reduced matrix density of A. If A and B denote the two electron spins, their entropies are equal for both spin functions $|\psi_{ABC}\rangle = |\psi_\pm\rangle$ while the entropy S_C of the nuclear spin is null. The calculation of $\log_2 \rho_A$ requires the diagonalization of the representative matrix of ρ_A. Figure 1 plots the variations of the entropy $S_{\frac{1}{2}(1)}$ with respect to the strength of the magnetic field. On approaching the resonances, their degree of entanglement increases and finally reaches a maximum at the resonances at which the two pure states are equally probable, i.e., $|c_{J\pm}|^2 = \frac{1}{2}$, with $J = 1$–2 (see Fig. 3 in Ref. 5). Taking into account the hyperfine coupling constant $A_\perp$ does not significantly reduce the degree of entanglement. Similar results have been found by the authors of Ref. 25, who studied the energy spectrum of hydrogen and sodium atoms.

B. Geometric phases

1. Tripartite system

The existence of phases of geometric character has been verified experimentally in various fields: Josephson-junction devices, quantum dots, ion traps, etc. A geometric phase is independent of how the transportation is executed. It can be adiabatic, nonadiabatic, cyclic, or noncyclic.[26] Quantum phase gates are expected to be robust against decoherence and have built-in fault tolerance features. They are the basis of geometric computation.[14]

In order to generate geometric phases, the sample is placed in a rotating magnetic field $H(t)$, directed along the unit vector $n = [\sin\theta\cos\varphi(t), \sin\theta\sin\varphi(t), \cos\theta]$. θ and $\varphi = \omega t$ are the azimuthal and polar angles in spherical coordinates, respectively. The angular frequency ω is assumed to be constant. In practice, one can use two magnetic fields, one parallel to the z axis and the other perpendicular to the z axis. The latter must be rotating. Below, we consider that the two defects are now lying along the same direction $\langle 111 \rangle$ and are separated by a slightly smaller distance than that given above, i.e., 11.58 Å (see also Ref. 4). The nitrogen atoms occupy substitutional positions. In this new configuration, the fine-structure coupling constant J_{yz} vanishes [see Eq. (3)]. The positions of the LAC in the Zeeman diagram depend on the relative position of the two defects and the additional parameters of the magnetic field, i.e., ω and θ. Since any initial state vector can gain a geometric phase, its general form $|\psi(0)\rangle = \sum_{m_S^{\mathrm{NV}}, m_S^N, m_I^N}(c_{m_S^{\mathrm{NV}}, m_S^N, m_I^N})|m_S^{\mathrm{NV}} m_S^N m_I^N\rangle$ is then considered below.

Under these conditions, the magnetically transported state vectors of the whole system $\psi(t) = e^{i\phi(t)}\psi(0)$ are solutions of the time-dependent Schrödinger equation, $\mathcal{H}[H(t)]\psi(t) = i\frac{d}{dt}\psi(t)$ ($\hbar = 1$). $\mathcal{H}$ is still the sum of $\mathcal{H}_1$ and the Zeeman operator $\mathcal{H}_Z$ [Eqs. (1) and (2)]. The total geometric phase acquired by the whole spin system can be obtained by removing the dynamical phase $-i\int_0^t\langle\psi(t')|\frac{d}{dt'}\psi(t')\rangle dt'$ from the total phase $\phi(t) = \arg\langle\psi(0)|\psi(t)\rangle$.[27] In order to obtain the exact solutions $\psi(t)$, an appropriate time-dependent unitary transformation $R(t)$ is required. In the case of isotropic or weak anisotropic spin-spin interactions (Breit-Rabi model, Heisenberg XY model, etc.) it is more convenient to consider transformations that lead to a diagonal and time-invariant Hamiltonian.[25,28,29] Here, the aim is to avoid the appearance of new off-block elements in the 18-dimensional energy matrix. We then consider a simple rotation through an angle φ about the z axis: $R(t) = e^{i\varphi(t)(S_z^{\mathrm{NV}}+S_z^N+I_z^N)}$.[30]

The transformed state vectors, $\psi'(t) = R(t)\psi(t)$, are also solutions of a Schrödinger equation, $\mathcal{H}'\psi'(t) = i\frac{d}{dt}\psi'(t)$, but the new Hamiltonian $\mathcal{H}' = R\mathcal{H}R^{-1} - iR\frac{d}{dt}R^{-1}$ is time independent:

$$\mathcal{H}' = \mathcal{H}_1 - \omega I_z^N + \Omega e \cdot (S^{\mathrm{NV}} + S^N) \tag{5}$$

In other words, the spin system feels an effective magnetic field $H_e = \Omega/g\mu_B$, with $\Omega = (\omega_L^2 + \omega^2 - 2\omega\omega_L\cos\theta)^{\frac{1}{2}}$. It is directed along the unit vector $e = (e_x, 0, e_z)$ and makes an angle $\vartheta = \arccos(\frac{\omega_L}{\Omega}\cos\theta - \frac{\omega}{\Omega})$ with the z axis. If the spin system evolves adiabatically ($\omega \ll \omega_L$), the frequency Ω tends towards the Larmor frequency and the effective angle ϑ tends towards θ, the actual inclination of the magnetic field with respect to the z axis.

The eigenstates of the time-invariant Hamiltonian are of the form $\psi'(t) = e^{-iE't}\psi'(0)$, and those of $\mathcal{H}$ are given by $\psi(t) = U(t)\psi(0)$, where $U(t) = R^{-1}(t)e^{-iE't}R(0)$ is the transport operator. The energy E', expressed in frequency units, and the initial state vector $\psi'(0) = \psi(0)$ are, respectively, the eigenvalue and eigenvector of the Schrödinger equation $\mathcal{H}'\psi'(0) = E'\psi'(0)$. Since $R(0) = -R(T) = I$, where $T = \omega/2\pi$ is a period and I is the identity operator, one can readily obtain the total geometric phase gained during a 2π rotation, namely, the
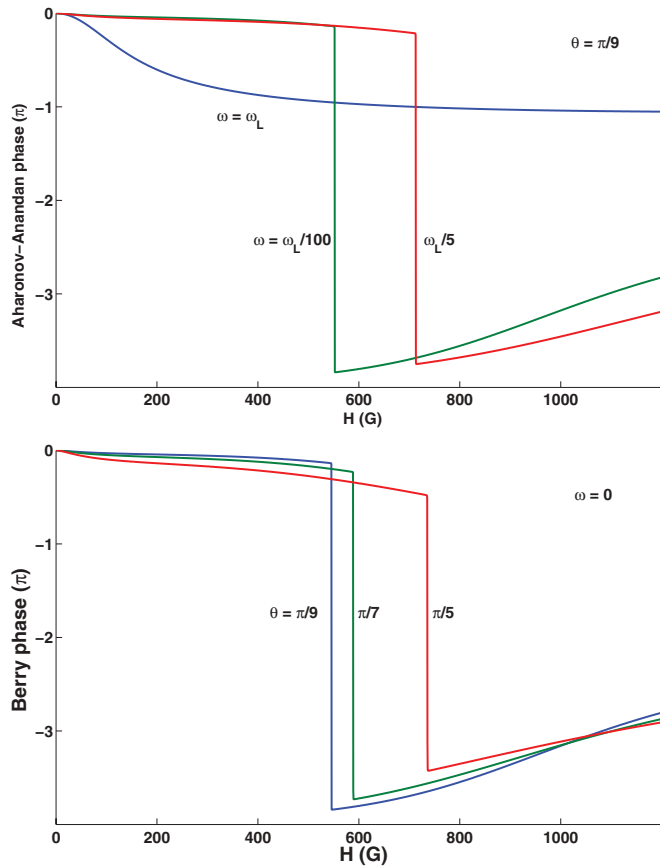
FIG. 2. (Color online) Variations of the cyclic geometric phases (in units of π) with respect to the strength of the magnetic field. ω and θ are, respectively, the rotational frequency of the magnetic field about the z axis and its inclination with respect to the same axis. ω_L is the Larmor frequency. (top) Nonadiabatic Aharonov-Anandan (AA) geometric phase. (bottom) The Berry phase.

nonadiabatic cyclic Aharonov-Anandan (AA) phase:

$$\phi_{AA} = 2\pi \left(-\frac{1}{2} + \sum_{m_S^{NV}, m_S^N, m_I^N} \left(m_S^{NV} + m_S^N + m_I^N \right) \left\| c_{m_S^{NV} m_S^N m_I^N} \right\|^2 \right) \tag{6}$$

The coefficients $c_{m_S^{NV} m_S^N m_I^N}$ of the state vector depend on the coupling constants involved in Eq. (1) and on the parameters of the magnetic field but not on φ, which is time dependent. It is not difficult to check the validity of Eq. (6): if only the spin $\frac{1}{2}$ is subjected to the rotating magnetic field, ϕ_{AA} reduces to the well-known result, i.e., half of the solid angle $\Phi = 2\pi(-1 \pm \cos\vartheta)$. If the spin system evolves very slowly ($\omega \to 0$), the AA phase tends to be identified with the Berry phase. Figure 2 shows the variations of the total geometric phases with respect to the magnetic field. Both the AA and Berry phases undergo almost 4π jumps at the resonances. Nevertheless, the geometric phase is 2π modular, and the experimentally detected jumps will not exceed 2π. According to some authors, the AA phase is more advantageous than the Berry phase in quantum computing.[31] The Berry phase has at least two drawbacks: it has a very slow evolution (while the coherence time is usually short), and it is accompanied by a dynamic component which is more fault tolerant.

2. Subsystems

The concept of geometric phase has been generalized to mixed states by two groups.[13,32] The Uhlmann geometric phase requires a purification and an attachment of an ancilla to the system. Below, we follow the approach of Sjöqvist *et al.*[13] which naturally extends the formalism developed above. For the initial state vector of the tripartite system $\psi(0) = \psi'(0) = \psi'_{ABC}(0)$, the marginal mixed-state geometric phase of the subsystem A is given by[13]

$$\gamma_A = \arg\left(\sum_j \lambda_j e^{i\beta_j} \right), \tag{7}$$

where the argument function returns an angle that lies between $\pm\pi$. λ_j are the eigenvalues of the reduced density operator $\rho_A(0) = \mathrm{Tr}_{BC}(|\psi'(0)\rangle\langle\psi'(0)|) = \sum_j \lambda_j |V_j(0)\rangle\langle V_j(0)|$, with $|V_j(0)\rangle = \sum_m a_m^j |m\rangle$. The ket $|m\rangle$ stands for the orthonormal basis of the subsystem A, i.e., $|m_S^{NV}\rangle$ or $|m_S^N\rangle$. The marginal density operator $\rho_A(0)$ evolves unitarily under the (unitary) transformation $R_A(\varphi) = e^{i\varphi S_z^A}$.[29,33] The geometric phase β_j of the individual pure state $|V_j\rangle$ can be obtained as shown above, i.e., by removing the dynamical phase from the total phase.[27] Consequently, the phase β_j is given by an equation similar to Eq. (6):

$$\beta_j = 2\pi \left(-\frac{1}{2} \delta_{S,\frac{1}{2}} + \sum_m m \left\| a_m^j \right\|^2 \right), \tag{8}$$

where $\delta_{S,\frac{1}{2}}$ is the Kronecker symbol. It is equal to 1 for spin $\frac{1}{2}$ and 0 for spin 1. Figure 3 plots the variations of the marginal geometric phases γ_1 and $\gamma_{\frac{1}{2}}$ with respect to the magnetic field. Once more, discontinuities occur at the resonances. On both sides of the jumps, the sum of γ_1 and $\gamma_{\frac{1}{2}}$ is rigorously equal to the Berry phase shown on Fig. 2. This equality is expected since we set $g^N = g^{NV}$ in Eq. (2).[29] The two independent
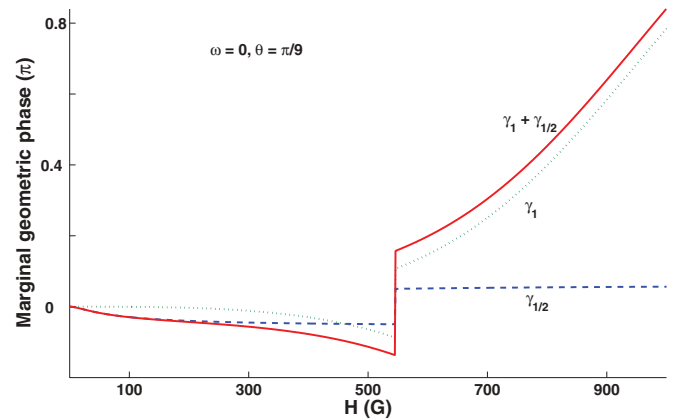

FIG. 3. (Color online) Variations of the marginal geometric phases (in units of π) acquired by the electron spins with respect to the strength of the magnetic field. The sum of γ_1 and $\gamma_{\frac{1}{2}}$ gives the Berry phase shown in Fig. 2. ω and θ are defined in the text and in Fig. 2.

components of g^N are equal to 2.0024 and differ only slightly from that of g^{NV} : $g_\parallel^{NV} = 2.0029$ and $g_\perp^{NV} = 2.0031$ (see Refs. 17 and 34). Using the simplest Hamiltonian, i.e., an isotropic coupling between two spins, $J \cdot S_1 \cdot S_2$, the authors of Ref. 29 showed that the above-mentioned equality is not verified if the g factors are different. We also note that the difference between the jump of $(\gamma_1 + \gamma_{\frac{1}{2}})$ and that of the Berry phase is equal to a multiple of 2π.

IV. CONCLUSION

We investigated the entanglement of the electron spins carried by the diamond NV$^-$-P1 coupled defect pair. We found that they are entangled in the immediate vicinity of the resonances at which two energy levels are closest to one another. The total geometric phase and the marginal geometric phases acquired, respectively, by the whole spin system and its subsystems have also been computed. At the resonant magnetic fields, entanglement is maximal, and the geometric phases undergo discontinuities. The interest in entanglement and topological phases is motivated by their applications in quantum information processing. This work extends a previous one which was focused on the spin flips that occur by quantum tunneling beyond the resonances. The next step is the investigation of the degree of entanglement of the spins at different LAC and for different relative positions of the two centers. The study of the properties of a large number of coupled centers is another goal.

[1] B. Kane, Nature (London) **393**, 133 (1998).

[2] J. Wrachtrup and F. Jelezko, J. Phys. Condens. Matter **18**, S807 (2006).

[3] T. Gaebel, M. Domhan, I. Popa, C. Wittmann, P. Neumann, F. Jelezko, J. R. Rabeau, N. Stavrias, A. D. Greentree, S. Prawer, J. Meijer, J. Twamley, P. R. Hemmer, and J. Wrachtrup, Nat. Phys. **2**, 408 (2006).

[4] R. Hanson, F. M. Mendoza, R. J. Epstein, and D. D. Awschalom, Phys. Rev. Lett. **97**, 087601 (2006).

[5] M. Hebbache, Phys. Rev. B **84**, 193204 (2011).

[6] K. Holliday, N. B. Manson, M. Glasbeek, and E. van Oort, J. Phys. Condens. Matter **1**, 7093 (1989).

[7] T. van der Sar, Z. H. Wang, M. S. Blok, H. Bernien, T. H. Taminiau, D. M. Toyli, D. A. Lidar, D. D. Awschalom, R. Hanson, and V. V. Dobrovitski, Nature (London) **484**, 82 (2012).

[8] A. M. Stoneham, A. H. Harker, and G. W. Morleyal, J. Phys. Condens. Matter **21**, 364222 (2009).

[9] E. Schrödinger, Naturwissenschaften **23**, 807 (1935); **23**, 823 (1935); **23**, 844 (1935).

[10] D. Deutsch, Proc. R. Soc. London, Ser. A **400**, 97 (1985).

[11] M. V. Berry, Proc. R. Soc. London, Ser. A **392**, 45 (1984).

[12] Y. Aharonov and J. Anandan, Phys. Rev. Lett. **58**, 1593 (1987).

[13] E. Sjöqvist, A. K. Pati, A. Ekert, J. S. Anandan, M. Ericsson, D. K. L. Oi, and V. Vedral, Phys. Rev. Lett. **85**, 2845 (2000).

[14] A. Ekert, M. Ericsson, P. Hayden, H. Inamori, J. A. Jones, D. K. L. Oi, and V. Vedrak, J. Mod. Opt. **47**, 2501 (2000).

[15] E. van Oort, P. Stroomer, and M. Glasbeek, Phys. Rev. B **42**, 8605 (1990).

[16] C. Kollmar and H. Sixl, Mol. Phys. **45**, 1199 (1982).

[17] S. Felton, A. M. Edmonds, M. E. Newton, P. M. Martineau, D. Fisher, D. J. Twitchen, and J. M. Baker, Phys. Rev. B **79**, 075203 (2009).

[18] J. H. N. Loubser and J. A. van Wyk, Rep. Prog. Phys. **41**, 1201 (1978).

[19] MATLAB, MATHEMATICA, and the f02haf FORTRAN routine of NAG library (under academic licenses).

[20] P. Neumann, N. Mizuochi, F. Rempp, P. Hemmer, H. Watanabe, S. Yamasaki, V. Jacques, T. Gaebel, F. Jelezko, and J. Wrachtrup, Science **320**, 1326 (2008); **323**, 1169 (2009).

[21] B. W. Lovett and S. C. Benjamin, Science **323**, 1169 (2009).

[22] D. Maclaurin, M. W. Doherty, L. C. L. Hollenberg, and A. M. Martin, Phys. Rev. Lett. **108**, 240403 (2012).

[23] S. Ryu and Y. Hatsugai, Phys. Rev. B **73**, 245115 (2006).

[24] R. Horodecki, P. Horodecki, M. Horodecki, and K. Horodecki, Rev. Mod. Phys. **81**, 865 (2009).

[25] S. Oh, Z. Huang, U. Peskin, and S. Kais, Phys. Rev. A **78**, 062106 (2008).

[26] *Geometric Phases in Physics*, edited by A. Shapere and F. Wilczek (World Scientific, Singapore, 1990).

[27] N. Mukunda and R. Simon, Ann. Phys. (NY) **228**, 205 (1993).

[28] X. Y. Jia, W. D. Li, and J. Q. Liang, Chin. Phys. **16**, 2855 (2007).

[29] M. L. Liang, S. L. Shu, and B. Yuan, Phys. Scr. **75**, 138 (2007).

[30] M. M. He, G. Chen, and J. Q. Liang, Eur. Phys. J. D **44**, 551 (2007).

[31] A. Blais, Ann. Phys. (Paris, Fr.) **28**, 1 (2003).

[32] A. Uhlmann, Lett. Math. Phys. **21**, 229 (1991).

[33] E. Sjöqvist, X. X. Yi, and J. Åberg, Phys. Rev. A **72**, 054101 (2005).

[34] In *Semiconductors: Impurities and Defects in Group IV Elements, IV-IV and III-V Compounds, Part a: Group IV Elements*, Landolt-Börnstein, New Series Vol. 41A2a, edited by O. Madelung, U. Rössler, and M. Schulz (Springer, Berlin, 2002).